British Journal of Hospital Medicine

Br. J. Hosp. Med. (Lond) **2026**; 87(4): 52966
https://doi.org/10.31083/BJHM52966

Article

Platelet-To-Lymphocyte Ratio and 28-Day Survival in Critically Ill Patients With Pulmonary Hypertension: Insights From a MIMIC-IV Retrospective Analysis

Dedong Ge[1], Zhengang Zhang[1,*]

[1]Department of Cardiology, Affiliated Hospital of Yangzhou University, Yangzhou University, 225001 Yangzhou, Jiangsu, China
*Correspondence: shyzdxfsyy@163.com (Zhengang Zhang)

Academic Editor: John Alcolado
Submitted: 30 May 2025 Revised: 27 July 2025 Accepted: 28 August 2025 Published: 16 April 2026

Abstract

Aims/Background: Existing pulmonary arterial hypertension (PAH) risk stratification, based on hemodynamics and functional parameters, is often inadequate in critical illness. The platelet-to-lymphocyte ratio (PLR), reflecting inflammatory and thrombotic pathways, may enhance outcome prediction. This study aimed to determine the prognostic value of PLR for 28-day mortality in critically ill PAH patients, evaluate nonlinear thresholds, and validate predictive performance using machine learning. **Methods**: A retrospective cohort of 1512 PAH patients was extracted from the Medical Information Mart for Intensive Care IV (MIMIC-IV) v3.0 database (2008–2022). PLR was derived from admission hematologic parameters. Multivariable Cox regression, restricted cubic spline (RCS) models, and machine learning algorithms were employed to assess associations between PLR and mortality. **Results**: RCS analysis revealed a U-shaped relationship with mortality, identifying critical thresholds: PLR $<$67.32 was associated with reduced risk, while PLR $>$75.92 indicated an abrupt risk escalation (adjusted hazard ratio (HR) = 2.261, 95% confidence interval (CI): 1.053–4.854, $p = 0.014$). Machine learning models incorporating PLR achieved moderate discrimination (concordance index [C-index] = 0.700). Subgroup analyses confirmed consistent prognostic value across age, sex, chronic kidney disease (CKD), and chronic obstructive pulmonary disease (COPD) subgroups (all p-interaction > 0.05). **Conclusion**: PLR represents an independent predictor of short-term mortality in critically ill PAH patients, with nonlinear thresholds offering actionable risk stratification. Integration of PLR into prognostic models may strengthen early risk assessment and guide timely interventions in critical care settings.

Keywords: pulmonary hypertension; platelet-to-lymphocyte ratio; critical illness; mortality; nonlinear threshold; prognostic models

1. Introduction

Pulmonary arterial hypertension (PAH) is a life-threatening disorder characterized by progressive vascular remodeling and elevated pulmonary artery pressure, associated with substantial morbidity and mortality despite therapeutic advances [1]. As a subtype of precapillary pulmonary hypertension, PAH has an estimated prevalence of 10–50 per 1 million population and represents a minority among pulmonary hypertension etiologies, where left heart disease predominates [2,3]. Definitive diagnosis requires right heart catheterization demonstrating a mean pulmonary artery pressure $\geq$25 mmHg and a pulmonary arterial wedge pressure $\leq$15 mmHg [4]. Although novel pulmonary vasodilators (e.g., endothelin receptor antagonists, phosphodiesterase-5 inhibitors, prostacyclin analogues) have improved outcomes, long-term survival remains suboptimal [2,3]. Current risk stratification strategies primarily rely on hemodynamic and functional parameters. However, these metrics exhibit limited sensitivity in critically ill patients experiencing dynamic clinical deterioration [5,6]. The identification of robust biomarkers that integrate inflammatory and thrombotic pathways may therefore enhance prognostic precision in intensive care settings [7,8].

The platelet-to-lymphocyte ratio (PLR), a composite index derived from routine hematologic measurements, has emerged as a potential prognostic biomarker in cardiovascular diseases, reflecting both thrombotic propensity and systemic inflammation [9,10]. Elevated PLR has been associated with adverse outcomes in chronic PAH cohorts. However, its predictive value in critically ill patients, particularly regarding nonlinear mortality associations, remains insufficiently explored [11]. Existing evidence is limited by single-center designs and inadequate adjustment for illness severity.

To address these gaps, we conducted a retrospective cohort study using the Medical Information Mart for Intensive Care IV (MIMIC-IV) 3.0 database (2008–2022) to evaluate the prognostic value of PLR in 1512 critically ill PAH patients. A multidimensional analytical framework incorporating survival analysis, restricted cubic spline modeling, and machine learning algorithms was applied to address three critical knowledge gaps: (1) the quantitative association between PLR and 28-day mortality, (2) the presence of nonlinear threshold effects in intensive care unit (ICU) populations, and (3) the stability of PLR's predictive performance across clinical subgroups.

This investigation addressed critical knowledge gaps in understanding the prognostic implications of PLR in critically ill PAH populations. Specifically, we examined the relationship between PLR levels and clinical outcomes and explored potential nonlinear associations. By employing complementary analytical approaches, we aim to evaluate the consistency of PLR's predictive capacity across diverse clinical endings, strengthening early risk assessment strategies and informing timely interventions in this vulnerable patient population.

2. Methods

2.1 Study Design and Data Source

This retrospective cohort study utilized the MIMIC-IV database (version 3.0; https://mimic.mit.edu/), which contains de-identified clinical records of more than 300,000 patients admitted to Beth Israel Deaconess Medical Center (Boston, MA, USA) between 2008 and 2022. Patients with PAH were identified using International Classification of Diseases (ICD) codes in conjunction with World Health Organization (WHO) diagnostic criteria [12]. Laboratory variables were extracted from each patient's first clinical measurement obtained within 24 hours of ICU admission, establishing baseline values for analysis. Structured Query Language (SQL) queries were used to retrieve demographics, time-stamped laboratory data (including platelet and lymphocyte counts for PLR calculation), vital signs, and clinical outcomes.

2.2 Inclusion and Exclusion Criteria

2.2.1 Inclusion Criteria

(a) Adult patients (aged 18–90 years) with PAH confirmed by standard diagnostic criteria [12].

(b) ICU admission records with complete first blood sample results (platelet count and lymphocyte count) obtained within 24 hours of ICU entry.

(c) The length of hospital stay in the ICU exceeds 24 hours.

2.2.2 Exclusion Criteria

(a) ICU stay shorter than 24 hours.

(b) Missing initial hematological measurements within the first 24 hours of ICU admission.

(c) Multiple ICU admissions (only the first admission episode included).

(d) Concurrent sepsis diagnosis defined by Sepsis-3 criteria [13]. Sepsis was excluded to ensure PAH remained the primary driver of critical illness, preventing confounding of PAH-specific manifestations and treatment responses.

(e) Active malignancy or a diagnosis of malignancy within the previous 5 years (excluding localized skin cancers).

(f) Documented hematological disorders with significant impact on blood counts (e.g., myeloproliferative neoplasms, myelodysplastic syndromes, primary immune thrombocytopenia, active hemolysis).

(g) Systemic immunosuppressive therapy (e.g., $>$10 mg/day prednisone equivalent, chemotherapeutic agents, biologics) prior to or during ICU admission.

(h) Known active autoimmune diseases (e.g., systemic lupus erythematosus, rheumatoid arthritis, scleroderma) or clinically evident systemic inflammatory conditions.

2.2.3 Laboratory Data Specificity

All hematologic parameters were derived exclusively from the first available measurement within 24 hours of ICU admission.

2.2.4 Final Cohort

Application of these criteria yielded a study population of 1512 critically ill patients with PAH.

2.2.5 Primary Endpoint

The primary endpoint was 28-day all-cause mortality, defined as death from any medical cause occurring within 28 days after ICU admission. This included fatal events related to pulmonary hypertension, comorbid conditions, or incidental triggers, regardless of hospital discharge status.

2.3 Data Preprocessing

Variables with $>$15% missingness were excluded prior to analysis, while variables with $\leq$15% missingness underwent multiple imputation using the IterativeImputer in scikit-learn (v1.2.2, https://github.com/scikit-learn/scikit-learn) with 10 iterations and Bayesian ridge regression. Imputation quality was validated rigorously: Kernel density plots confirmed near-identical distributions between observed and imputed values across variables, and scatterplots demonstrated preserved correlation structures.

Outliers were detected using interquartile range (IQR) thresholds and visually confirmed by boxplot analysis. Continuous variables were normalized using Z-score transformation, while non-normally distributed data underwent logarithmic transformation. PLR was calculated as platelet count ($\times 10^3/\mu$L) divided by absolute lymphocyte count ($\times 10^3/\mu$L) [6].

2.4 Statistical Analysis

2.4.1 Baseline Characteristics

Patients were stratified by PLR tertiles (Tertile 1 [T1]: 1.10–105.42, Tertile 2 [T2]: 105.52–235.82, Tertile 3 [T3]: 237.24–5300). Distributional normality of continuous variables was evaluated using the Shapiro-Wilk test. All parameters were non-normally distributed (normality rejected at $p < 0.05$). Intergroup comparisons of baseline characteristics were performed using the nonparametric Kruskal-Wallis test, with results expressed as medians and interquartile ranges (IQRs). Categorical variables were reported as

frequencies and percentages [n, (%)] and compared using χ^2 tests as appropriate.

2.4.2 Survival Analysis

Kaplan-Meier curves were generated to visualize 28-day survival probabilities across PLR tertiles, with survival differences evaluated by log-rank tests. The discriminative performance of multivariable Cox regression models was quantified using Harrell's concordance index (C-index), which estimated the probability that a randomly selected patient who died had a higher predicted risk than one who survived.

2.4.3 Multivariable Modeling

Cox proportional hazards models were used to evaluate predictors of 28-day mortality. Candidate variables were selected based on:

Clinical relevance: Sequential Organ Failure Assessment (SOFA) score (organ failure severity), age, and sex (established predictors in critical illness).

Cardiorespiratory status: systolic blood pressure (SBP), heart rate, respiratory rate (RR), and oxygen saturation (SpO_2), reflecting hemodynamic and respiratory compromise in PAH.

Key comorbidities: chronic kidney disease (CKD) and chronic obstructive pulmonary disease (COPD), both known to exacerbate PAH progression and mortality.

Biological rationale: weight was included as a surrogate for nutritional status and fluid balance.

Multicollinearity control was controlled by excluding variables with a variance inflation factor (VIF) $\geq$2; retained variables had VIF $<$2 (**Supplementary Table 1**). After clinical relevance assessment, biologic rationale, and VIF screening, final covariates adjusted in Cox models are presented in the multivariate regression analysis section of the Results.

2.4.4 Nonlinear Analysis

Restricted cubic splines (RCSs) with three knots (optimized by Akaike information criterion [AIC]) were employed to examine nonlinear associations between PLR and mortality. Threshold effects were quantified by χ^2 decomposition, with nonlinearity confirmed via likelihood ratio tests ($p < 0.05$).

2.4.5 Machine Learning

Feature selection was performed using the Boruta algorithm with 100 iterations and Bonferroni correction, identifying 15 predictive features from 27 candidate variables. Stratified random sampling preserved the distribution of the target outcome (28-day mortality) across training and test sets (70% and 30%, respectively). Class imbalance was addressed using Stratified ShuffleSplit in scikit-learn (v1.2.2).

Hyperparameters were calibrated through manual tuning to balance interpretability and complexity. Decision tree structure depth was restricted to three levels, prioritizing clinically interpretable decision paths while limiting overfitting. Minimum leaf samples (1) and split size (2) retained default values to capture granular mortality signals. Ensemble design comprised 100 decision trees, providing stable predictions without excessive computational burden ($<$1% area under the curve [AUC] gain beyond 500 trees). Reproducibility was ensured by fixed randomization (random_state = 1).

2.4.6 Statistical Validation of Model Significance

Model validity was assessed using three inferential frameworks. Joint covariate significance was determined via likelihood ratio testing, contrasting saturated models with intercept-only models. Wald statistics quantified partial effects of individual predictors, with emphasis on PLR-derived risk estimators. Log-rank procedures examined concordance between risk-stratified groups and survival timelines without parametric assumptions. All inferences used a two-tailed significance threshold of $\alpha = 0.05$.

2.4.7 Subgroup Analysis

Stratified Cox models were applied to evaluate effect modification using key variables. Age ($<$65 vs. $\geq$65 years) was dichotomized according to the WHO definition of "older adult" to reflect the increased comorbidity burden in PAH. Sex was included based on prior evidence of sex-specific outcome differences [14]. CKD and COPD were examined due to their prevalence in PAH and their potential to exacerbate systemic inflammation [15]. Interaction terms were tested using likelihood ratio tests.

2.4.8 Software

All analyses were conducted in R version 4.2.1 (R Foundation for Statistical Computing, Vienna, Austria) with the packages survival, rms, and random forest. Graphical and statistical representations were generated using the following open-source packages within the R environment: survminer (version 0.4.9, Kaplan-Meier survival curves, Alboukadel Kassambara, Montpellier, France), rms (v6.7-0, restricted cubic splines, Frank E. Harrell Jr., Vanderbilt University, Nashville, TN, USA), Boruta (v8.0.0, variable importance plots, Miron B. Kursa, Warsaw University of Life Sciences, Warsaw, Poland), pROC (v 1.18.4, receiver operating characteristic curves, Xavier Robin, University of Paris, Paris, France), forestplot (v3.1.1, subgroup analysis forest plots, Max Gordon, University of Auckland, Auckland, New Zealand). Statistical significance was defined as two-tailed $\alpha = 0.05$.

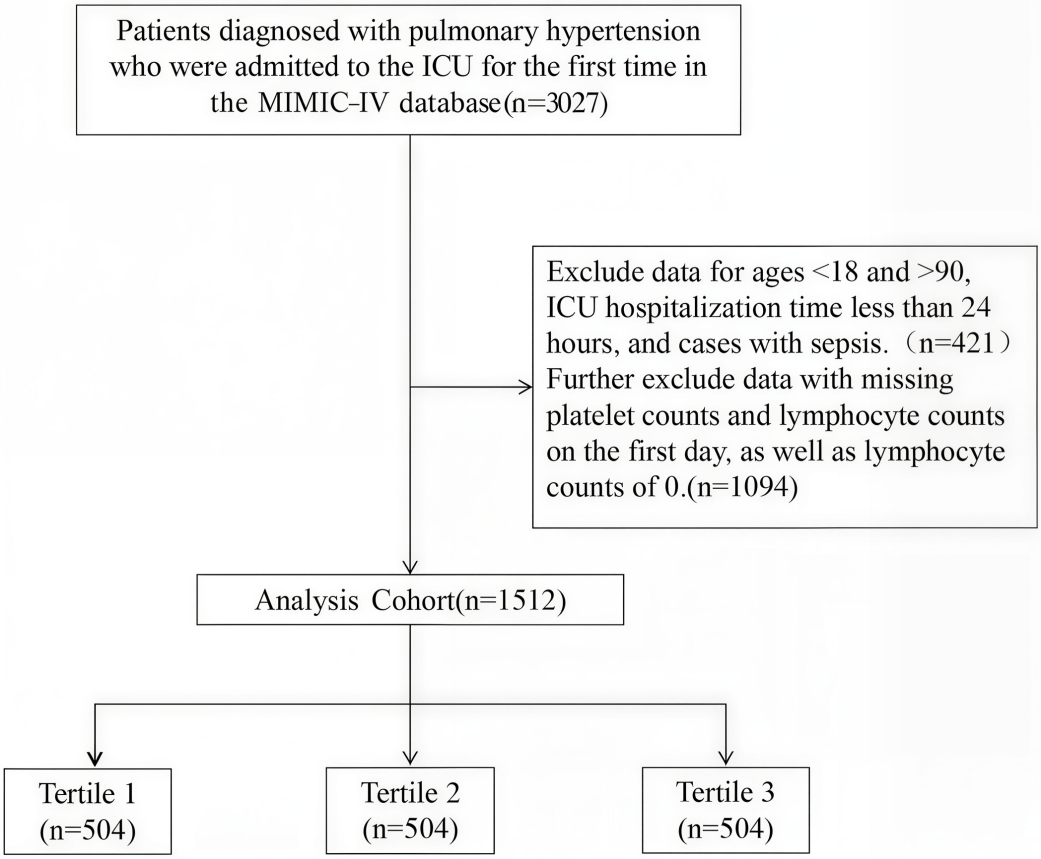

Fig. 1. Workflow for selection of the study population from the MIMIC-IV database. ICU, intensive care unit; MIMIC-IV, Medical Information Mart for Intensive Care IV.

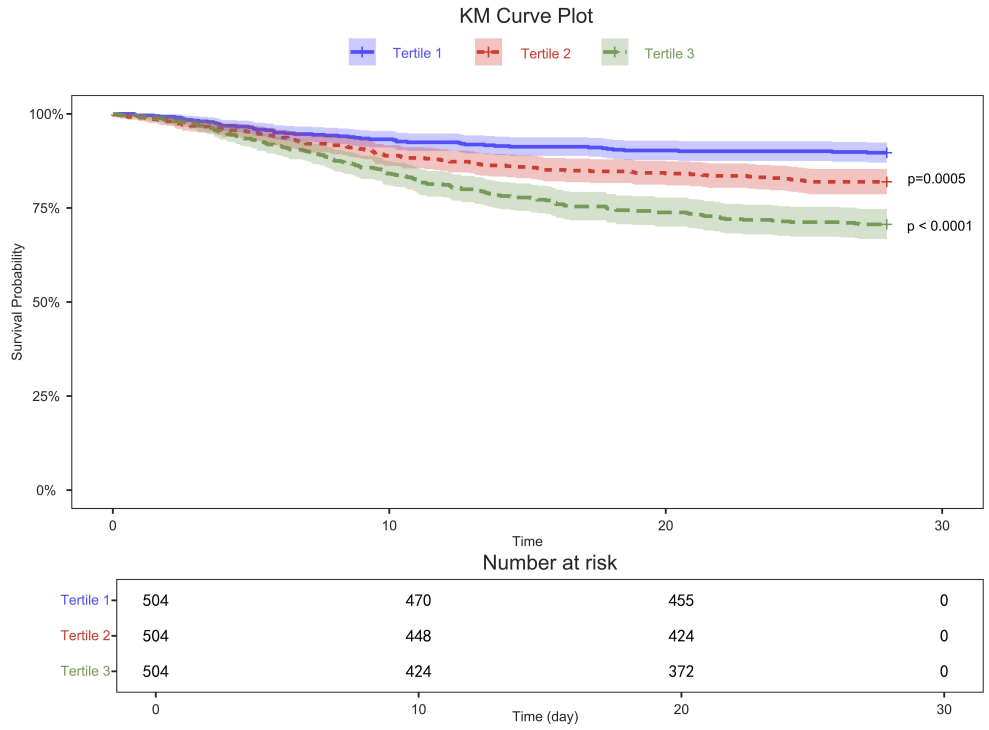

Fig. 2. Kaplan-Meier (KM) survival curves for 28-day outcomes in patients with pulmonary arterial hypertension. Survival rates are shown by platelet-to-lymphocyte ratio (PLR) tertiles: Tertile 1 (1.10–105.42), Tertile 2 (105.52–235.82), Tertile 3 (237.24–5300).

3. Results

3.1 Study Population and Baseline Characteristics

A total of 1512 critically ill PAH patients (Fig. 1) were identified from the MIMIC-IV 3.0 database (2008–2022) and stratified into PLR tertiles (T1: 1.10–105.42, T2: 105.52–235.82, T3: 237.24–5300) [16]. Baseline analysis revealed significant associations between PLR levels and multiple clinical indicators (Table 1). Compared with patients in the lowest tertile (T1), those in the highest tertile (T3) exhibited elevated cardiorespiratory markers, including increased heart rate and respiratory rate ($p < 0.001$), along with reduced oxygen saturation ($p < 0.001$). Indicators of organ dysfunction were also pronounced, with lower SOFA scores ($p < 0.001$), reduced lactate concentrations ($p < 0.001$), and reduced arterial partial pressure of arterial oxygen (PaO_2) ($p < 0.001$). Hematologic alterations were evident, characterized by higher platelet counts, decreased lymphocyte levels ($p < 0.001$), elevated red cell distribution width ($p < 0.001$), and higher absolute neutrophil counts ($p = 0.004$).

Metabolic and biochemical disturbances were also associated with higher PLR, including increased glucose levels ($p < 0.001$), elevated blood urea nitrogen ($p < 0.001$), increased serum creatinine ($p < 0.001$), and lower total bilirubin concentrations ($p < 0.001$). Comorbid conditions were more prevalent in patients with elevated PLR, with CKD (44.25% vs. 26.19%) and COPD (37.90% vs. 17.06%) occurring significantly more frequently ($p < 0.001$).

Notably, mortality outcomes differed substantially across tertiles. T3 patients demonstrated significantly higher in-hospital mortality ($p < 0.001$) and 28-day all-cause mortality ($p < 0.001$) compared to those in T1.

3.2 Survival Analysis and Mortality Outcomes

Kaplan-Meier analysis (Fig. 2) demonstrated significant divergence in survival curves across PLR tertiles (log-rank $p < 0.05$). The 28-day cumulative survival rate was markedly lower in the highest PLR tertile, with mortality reaching 29.37% compared to 10.32% in the lowest tertile ($p < 0.001$).

In multivariable Cox regression models, adjustments were made for sex, age, weight, CKD, COPD, heart rate, respiratory rate, systolic blood pressure, SpO_2, and SOFA score. Cox regression revealed a dose-dependent mortality risk (Table 2). Unadjusted models showed a 3.102-fold increased hazard in the highest PLR tertile (hazard ratio (HR) = 3.102, 95% confidence interval (CI): 2.253–4.271, $p < 0.001$), which persisted after full adjustment for covariates (adjusted HR = 3.047, 95% CI: 2.160–4.298; C-index = 0.733, $p < 0.001$). Similar results were observed for 28-day all-cause mortality (adjusted HR = 3.064, 95% CI: 2.180–4.305, C-index = 0.723, $p < 0.001$) (Table 3).

3.3 Nonlinear Association and Threshold Effects

Restricted cubic spline analyses revealed nonlinear associations between PLR and mortality outcomes in critically ill PAH patients. For in-hospital mortality (Fig. 3A,B), the unadjusted model identified an optimal inflection point at PLR = 75.92. Below this value, mortality risk plateaued, while above it, risk increased significantly (HR = 2.967, 95% CI: 1.448–6.078, $p < 0.001$) (**Supplementary Table 2**). After adjustment for sex, age, weight, comorbidities (CKD, COPD), and physiological parameters (heart rate, respiratory rate, SpO_2, systolic blood pressure, SOFA score), this PLR threshold remained associated with elevated mortality risk (adjusted HR = 2.261, 95% CI: 1.053–4.854, $p = 0.014$) (**Supplementary Table 2**). However, the overall nonlinear association became nonsignificant in the adjusted model ($p = 0.126$) (**Supplementary Table 3**).

For 28-day all-cause mortality, PLR demonstrated a robust U-shaped association ($p < 0.001$; Fig. 3C,D). The unadjusted model identified a threshold at PLR = 67.32, below this threshold, mortality risk decreased as PLR increased; above it, risk rose sharply with increasing PLR (unadjusted HR = 4.155, 95% CI: 2.731–6.322, $p < 0.001$) (**Supplementary Table 4**). This threshold remained predictive for 28-day mortality after multivariable adjustment (adjusted HR = 3.787, 95% CI: 2.431–5.898, $p < 0.001$) (**Supplementary Table 4**), confirming PLR as an independent risk stratification marker.

Covariate analyses identified SOFA score (HR = 2.004), age (HR = 1.365), and admission heart rate (HR = 1.277) as significant predictors of increased mortality (all $p < 0.05$), while SpO_2 exhibited a protective effect (HR = 0.875) (**Supplementary Table 5**). Both adjusted and unadjusted models demonstrated consistent knot placement (26.96–943.58) and strong nonlinear associations (χ^2 = 40.192 adjusted; χ^2 = 56.371 unadjusted), supporting model robustness. These findings provide quantifiable PLR thresholds tailored to specific mortality outcomes, enabling clinical risk stratification and personalized management (**Supplementary Table 6**).

3.4 Machine Learning Model Performance

Feature selection using the *Boruta* algorithm was performed on 27 clinical and laboratory parameters to evaluate PLR and other predictors of 28-day mortality among critically ill PAH patients. After 100 importance iterations with Bonferroni correction ($\alpha = 0.01$), 15 significant predictive features were identified (Fig. 4A).

A random forest machine learning model incorporating these variables demonstrated the predictive capacity of PLR for short-term mortality risk. Discrimination was assessed via receiver operating characteristic (ROC) curve analysis, with AUC and 95% CI used to quantify diagnostic accuracy in distinguishing survivors from non-survivors at 28 days. The ROC analysis revealed an AUC of 0.759 (95% CI: 0.708–0.810, $p < 0.001$, Fig. 4B). PLR-associated risk

Table 1. Baseline characteristics of the study population.

Variable	Levels	Overall (n = 1512)	PLR			H/χ^2	*p*-value
			T1 (n = 504)	T2 (n = 504)	T3 (n = 504)		
Heart rate (beats/min)		85 (75–99.5)	81 (75–91)	85 (73–99)	90 (77–105.5)	32.03	<0.001
Respiratory rate (breaths/min)		19 (15–24)	16 (14–20)	20 (16–24)	22 (17–26)	147.7	<0.001
SpO_2 (%)		98 (94–100)	99 (96–100)	97 (94–100)	96 (93–99)	108.93	<0.001
SBP (mmHg)		114 (100–131)	111.5 (99–125.5)	115 (101–132)	116 (100–135)	9.6	0.008
SOFA score		5.00 (3.00–8.00)	7.00 (5.00–9.00)	5.00 (3.00–8.00)	5.00 (3.00–7.00)	86.39	<0.001
Age (years)		73 (63–80)	70 (60–78)	72 (61.5–81)	75 (65.5–83)	34.91	<0.001
Weight (kg)		80.30 (66–97.05)	81.95 (69.03–95.98)	81.3 (66.35–100.05)	76.35 (62.73–95.2)	12.78	0.002
PLR		160.39 (84.13–292.99)	63.97 (44.23–84.13)	160.39 (127.5–191.66)	382.32 (292.99–527.37)	1343.11	<0.001
RDW (%)		15.4 (13.9–17.3)	14.5 (13.3–16)	15.5 (14.1–17.6)	15.9 (14.6–17.8)	101.14	<0.001
WBC (10^9/L)		11.30 (8.00–16.00)	12.20 (8.60–16.40)	10.70 (7.55–15.20)	11.40 (8.00–16.25)	11.62	0.003
ANC (10^9/L)		9.21 (6.08–13.21)	9.25 (6.18–13.45)	8.48 (5.65–12.24)	9.71 (6.53–13.71)	10.84	0.004
Total calcium (mg/dL)		8.50 (8.00–8.90)	8.30 (7.90–8.80)	8.60 (8.10–9.00)	8.50 (8.10–9.00)	20.11	<0.001
Glucose (mg/dL)		127 (107–160)	122.5 (106–146)	125 (104–158)	138 (112.5–177.5)	33.65	<0.001
Potassium (mmol/L)		4.30 (3.90–4.80)	4.30 (4.00–4.70)	4.30 (3.80–4.80)	4.30 (3.90–4.90)	1.35	0.508
iCa^{2+} (mmol/L)		1.12 (1.06–1.17)	1.12 (1.07–1.19)	1.11 (1.06–1.16)	1.12 (1.07–1.17)	5.46	0.065
Lactate (mmol/L)		1.70 (1.20–2.50)	2.00 (1.40–2.70)	1.60 (1.20–2.40)	1.60 (1.10–2.30)	33.84	<0.001
PaO_2 (mmHg)		82 (43–237.5)	254 (64.5–346.5)	72 (39.5–148)	62 (41–106)	208.06	<0.001
APTT (sec)		31.50 (27.80–39.30)	31.65 (27.85–38.10)	31.9 (28–43.25)	30.8 (27.6–38.3)	7.36	0.025
Total bilirubin (mg/dL)		0.70 (0.40–1.20)	0.80 (0.50–1.45)	0.70 (0.40–1.20)	0.60 (0.40–1.00)	45.7	<0.001
Serum creatinine (mg/dL)		1.20 (0.80–2.00)	1.00 (0.80–1.50)	1.30 (0.90–2.10)	1.40 (0.90–2.30)	58.87	<0.001
BUN (mg/dL)		26 (16–45)	19 (14–30)	27 (17–46)	33 (20.5–53.5)	120.85	<0.001
LDH (U/L)		306 (232–439.5)	338 (253–472)	299.5 (221–417)	288.5 (224.5–429.5)	20.63	<0.001
PLT (10^9/L)		171 (122.5–241)	122.5 (90–151)	182 (139.5–233.5)	239 (180–298)	479.1	<0.001
ALC (10^9/L)		1.11 (0.67–1.77)	2.00 (1.43–2.67)	1.17 (0.86–1.47)	0.58 (0.38–0.81)	813.45	<0.001
Sex (%)	Female	742.00 (49.07%)	230.00 (45.63%)	248.00 (49.21%)	264.00 (52.38%)	4.59	0.101
	Male	770.00 (50.93%)	274.00 (54.37%)	256.00 (50.79%)	240.00 (47.62%)		
CKD (%)	No	954.00 (63.10%)	372.00 (73.81%)	301.00 (59.72%)	281.00 (55.75%)	38.98	<0.001
	Yes	558.00 (36.90%)	132.00 (26.19%)	203.00 (40.28%)	223.00 (44.25%)		
COPD (%)	No	1105.00 (73.08%)	418.00 (82.94%)	374.00 (74.21%)	313.00 (62.10%)	56.08	<0.001
	Yes	407.00 (26.92%)	86.00 (17.06%)	130.00 (25.79%)	191.00 (37.90%)		
In-hospital mortality (%)	No	1236.00 (81.75%)	453.00 (89.88%)	422.00 (83.73%)	361.00 (71.63%)	58.27	<0.001
	Yes	276.00 (18.25%)	51.00 (10.12%)	82.00 (16.27%)	143.00 (28.37%)		
28-day all-cause mortality (%)	No	1221.00 (80.75%)	452.00 (89.68%)	413.00 (81.94%)	356.00 (70.63%)	59.52	<0.001
	Yes	291.00 (19.25%)	52.00 (10.32%)	91.00 (18.06%)	148.00 (29.37%)		

PLR: Tertile 1 (T1: 1.10–105.42), Tertile 2 (T2: 105.52–235.82), Tertile 3 (T3: 237.24–5300).

PLR, platelet-to-lymphocyte ratio; SpO_2, oxygen saturation; SBP, systolic blood pressure; SOFA, Sequential Organ Failure Assessment; RDW, Red Blood Cell Distribution Width; WBC, white blood cell; ANC, absolute neutrophil count; PaO_2, partial pressure of arterial oxygen; APTT, Activated Partial Thromboplastin Time; BUN, blood urea nitrogen; LDH, lactate dehydrogenase; PLT, platelet; ALC, absolute lymphocyte count; CKD, chronic kidney disease; COPD, chronic obstructive pulmonary disease; iCa^{2+}, ionized calcium.

Table 2. Cox regression model for in-hospital mortality.

PLR	Unadjusted HR (95% CI)	*p*-value	PLR	Adjusted HR (95% CI)	Adjusted *p*-value
T1	Reference		T1	Reference	
T2	1.667 (1.175–2.364)	0.004	T2	1.787 (1.243–2.569)	0.002
T3	3.102 (2.253–4.271)	<0.001	T3	3.047 (2.16–4.298)	<0.001

HR, hazard ratio; CI, confidence interval.

Table 3. Cox regression model for 28-day all-cause mortality.

PLR	Unadjusted HR (95% CI)	*p*-value	PLR	Adjusted HR (95% CI)	Adjusted *p*-value
T1	Reference		T1	Reference	
T2	1.818 (1.293–2.556)	0.001	T2	1.928 (1.355–2.743)	<0.001
T3	3.125 (2.278–4.286)	<0.001	T3	3.064 (2.18–4.305)	<0.001

Unadjusted model, Cox proportional hazards regression without covariate adjustment; Adjusted model, multivariable Cox regression adjusted for covariates; HR (95% CI), hazard ratio with 95% confidence interval; Reference group, T1 (lowest PLR tertile). T1 = 1.10–105.42; T2 = 105.52–235.82; T3 = 237.24–5300.

scores showed strong correlation with mortality, with a hazard ratio (HR) of 1.198 per unit increase (95% CI: 1.131–1.270; $p < 0.001$), corresponding to 19.8% elevated mortality risk for each incremental rise in PLR (**Supplementary Table 7**). The model exhibited moderate discriminative ability (C-index 0.700, Standard Error (SE) = 0.026), with overall validity confirmed by likelihood ratio, Wald, and Score tests (all $p < 0.001$) (**Supplementary Table 8**).

3.5 Subgroup Analysis

Subgroup analyses (Fig. 5) using Cox regression models demonstrated consistent associations between elevated PLR tertiles and increased 28-day mortality across age, sex, CKD, and COPD subgroups in critically ill PAH patients, with no statistically significant interaction effects (*p*-interaction > 0.05 for all). Patients aged $\geq$65 years in the highest PLR tertile (T3) exhibited an HR of 3.187 (95% CI: 2.162–4.697), while those <65 years showed a comparable HR of 2.956 (1.507–5.800). Similarly, male patients in T3 had an HR of 3.691 (2.379–5.727) compared with 2.940 (1.751–4.937) in females, though sex-based effect modification was nonsignificant ($p = 0.929$).

Comorbidity-stratified analyses revealed elevated mortality risks for T3 PLR among CKD patients (HR = 3.022, 95% CI: 1.733–5.27) and COPD patients (HR = 5.328, 95% CI: 2.589–10.966), yet neither interaction term reached statistical significance ($p = 0.773$ and 0.312, respectively). Forest plots confirmed uniform risk gradients across subgroups, with overlapping confidence intervals underscoring the stable prognostic value of PLR. Collectively, elevated PLR independently predicted 28-day mortality in severe PAH without significant modification by age, sex, or cardiopulmonary comorbidities.

4. Discussion

This retrospective cohort study elucidated the nonlinear threshold effects of PLR on 28-day mortality in critically ill adults with PAH, leveraging comprehensive clinical data from the MIMIC-IV 3.0 database. Our findings reveal that elevated PLR levels correlate with adverse hemodynamic and laboratory profiles, including increased heart rate, respiratory rate, and markers of end-organ dysfunction such as elevated total bilirubin and lactate dehydrogenase. These associations are consistent with the established interplay between systemic inflammation, coagulation abnormalities, and disease progression in PAH [17,18].

Univariate analysis demonstrated a strong association between PLR tertiles and 28-day mortality ($\chi^2 = 59.52$, $p < 0.001$; Table 1). Multivariable adjustment and restricted cubic spline analysis further identified a nonlinear threshold effect of PLR on mortality risk, with attenuation of the adjusted hazard ratio after controlling for SOFA score and other confounders. These findings suggest that simple group comparisons may overestimate the predictive value of PLR. Although continuous PLR analysis remained statistically significant ($p < 0.001$), its clinical relevance was limited (HR = 1.001, **Supplementary Table 9**). These findings support adopting threshold-based stratification, which more effectively identifies high-risk patients (T3 HR = 3.064) and provides clear targets for clinical intervention.

The nonlinear relationship between PLR and in-hospital mortality highlights a critical threshold effect. The unadjusted model identified a PLR threshold of 75.92, beyond which mortality risk rose sharply. The loss of significance in the nonlinear association after covariate adjustment ($p = 0.126$) may reflect mediation by SOFA score, age, and oxygenation. Although covariate adjustment attenuated this association, the persistence of a U-shaped relationship for 28-day all-cause mortality, with a consistent threshold at 67.32, suggests that PLR remains an independent prognostic marker. This dual-phase association implies that both extremes of PLR, whether reflecting severe thrombocytosis with lymphopenia or profound thrombocy-

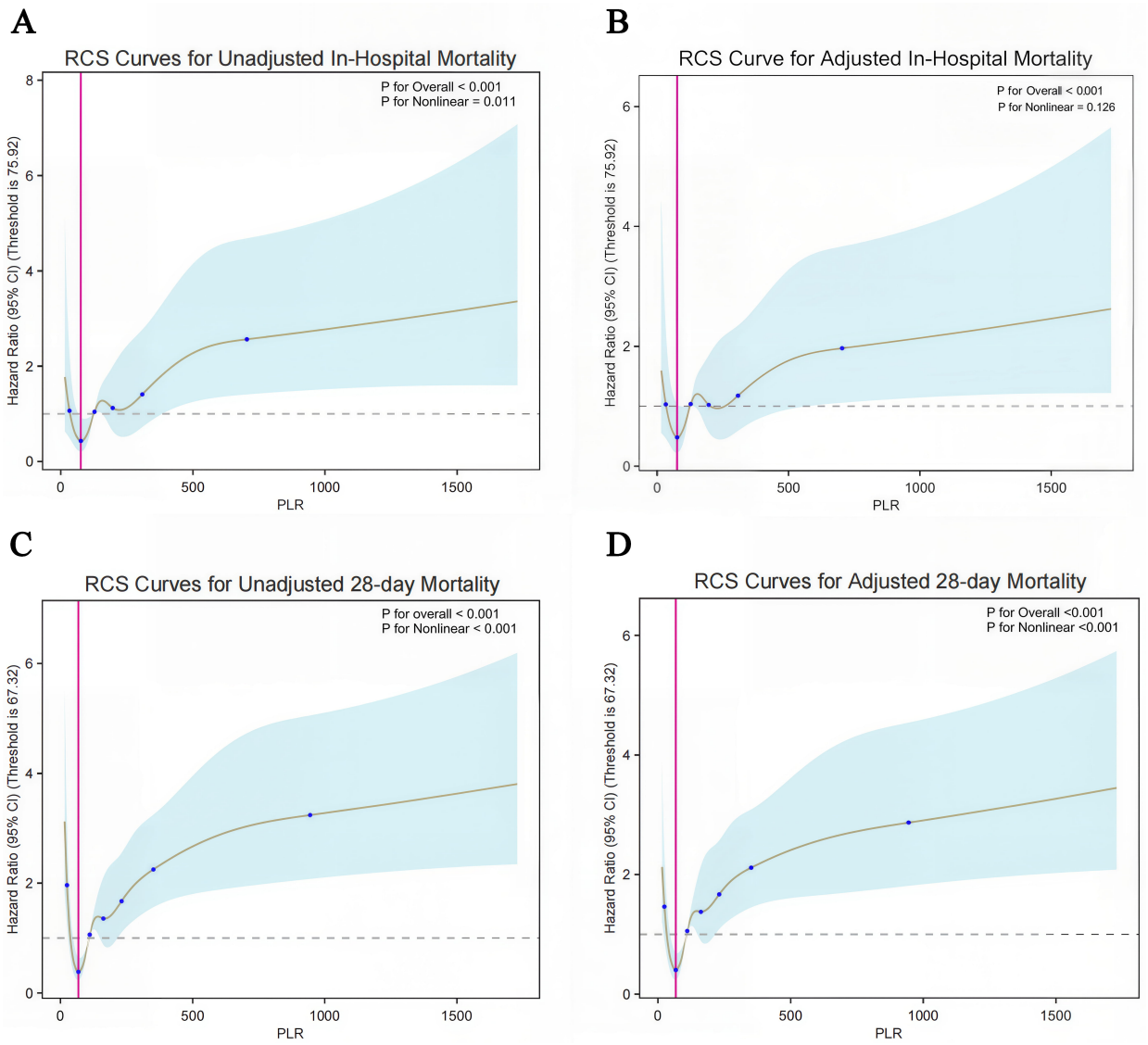

Fig. 3. Nonlinear association between PLR and 28-day all-cause mortality in pulmonary arterial hypertension (PAH). (A) Restricted cubic spline (RCS) curve for in-hospital mortality without covariate adjustment. (B) RCS curve for in-hospital mortality adjusted for confounders. (C) RCS curve for 28-day all-cause mortality without multivariable adjustment. (D) RCS curve for 28-day all-cause mortality with covariate adjustment. Shaded areas indicate 95% confidence intervals. Vertical red lines denote threshold values corresponding to minimal hazard ratios (HRs), while horizontal dashed lines represent the reference HR of 1.0. Covariates adjusted in multivariable models included sex, age, weight, comorbidities, heart rate, respiratory rate, systolic blood pressure, oxygen saturation, and Sequential Organ Failure Assessment (SOFA) score. Details of covariate selection rationale are provided in Multivariable Modeling section (consistent with the previous multivariate regression analysis).

topenia, may signify distinct pathophysiological states contributing to mortality [6,19]. The reduced significance of the nonlinear relationship after adjusting for covariates such as SOFA score, age, and SpO_2 highlights the multifactorial determinants of mortality in PAH; PLR likely interacts with systemic inflammation and organ dysfunction.

This study is the first to establish mortality risk thresholds for PLR (67.32 and 75.92) in critically ill PAH patients. These cutoff values likely represent distinct pathophysiological states. Values below the threshold may reflect preserved lymphocyte function and relative immune homeostasis, potentially contributing to improved survival [20]. Conversely, values exceeding the threshold suggest a vicious cycle of platelet activation and lymphocyte depletion, overlapping with the PLR range observed in PAH-related thromboinflammatory processes and multiorgan failure in critical illness [7,21].

Machine learning validation further corroborated the predictive value of PLR. The random forest model, incorporating PLR and 14 other clinically relevant features, demonstrated moderate discriminative performance (AUC: 0.759), with PLR-associated risk scores independently pre-

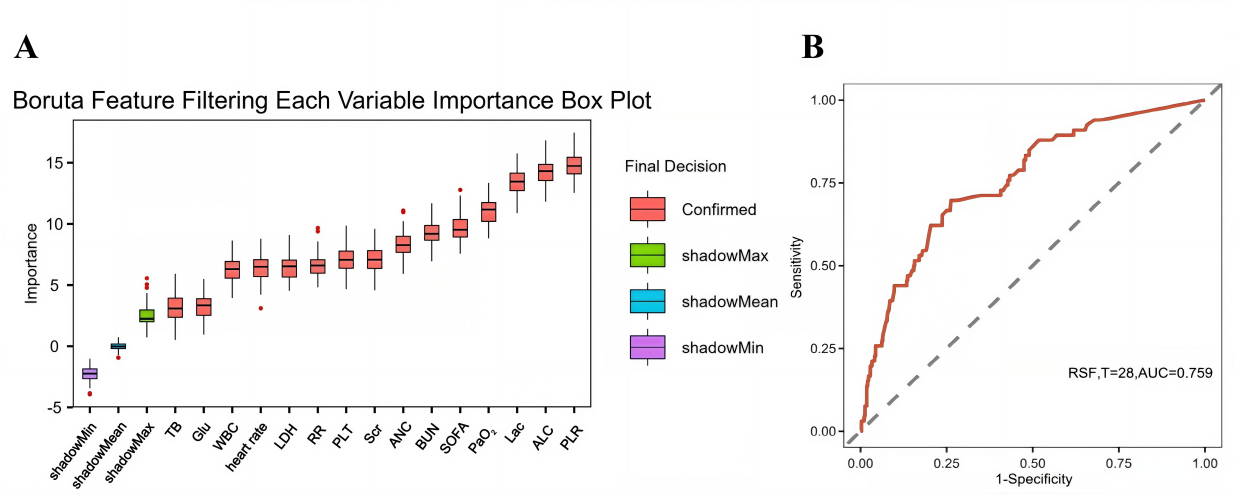

Fig. 4. Receiver operating characteristic (ROC) curve analysis of the random survival forest (RSF) machine learning model. (A) Variable importance assessment by the Boruta algorithm. The X-axis shows variable names, while the Y-axis shows corresponding Z-scores. Boxplots depict the distribution of Z-scores across 1000 iterations. Predictors were categorized as significant (red boxes) or nonsignificant (green boxes) based on permutation importance thresholds. (B) ROC curve showing RSF performance for time-to-event prediction (days). TB, total bilirubin; Glu, blood glucose; WBC, white blood cell; LDH, lactate dehydrogenase; RR, respiratory rate; PLT, platelet; Scr, serum creatinine; ANC, absolute neutrophil count; BUN, blood urea nitrogen; SOFA, Sequential Organ Failure Assessment; PaO_2, partial pressure of arterial oxygen; Lac, blood lactate; ALC, absolute lymphocyte count; PLR, platelet-to-lymphocyte ratio; AUC, area under the curve; RSF, random survival forest.

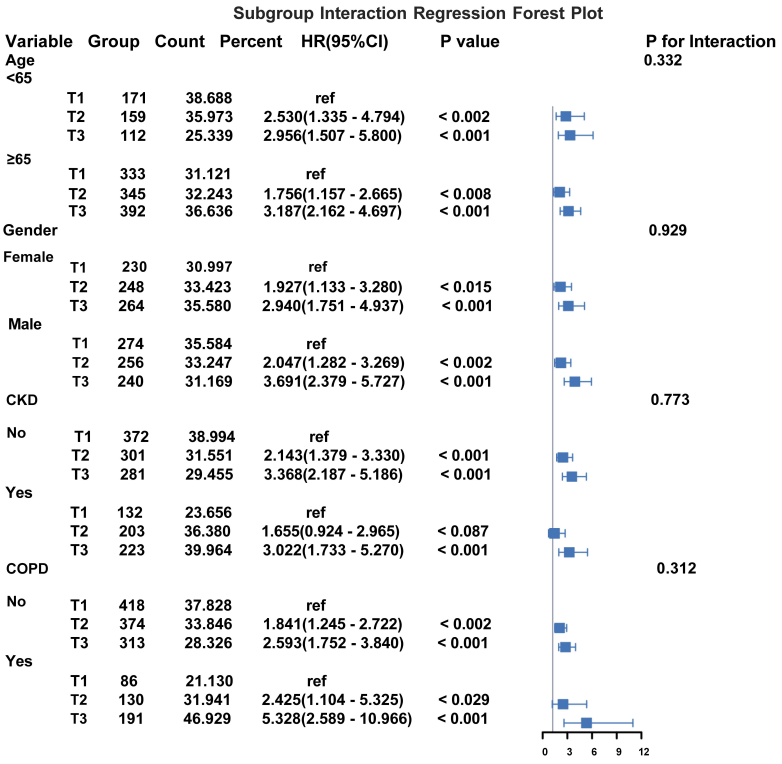

Fig. 5. Forest plot of subgroup interaction analyses for 28-day all-cause mortality. The multivariable Cox model was adjusted for confounders, including body weight, heart rate, respiratory rate, systolic blood pressure, and SOFA score. Hazard ratios (HRs) with 95% confidence intervals (CIs) are shown. Group column denotes tertile stratification: Tertile 1 (T1), Tertile 2 (T2), and Tertile 3 (T3), representing ordered subgroups by distribution of the exposure variable. ref, reference.

dicting a 19.8% increase in mortality per unit rise. This observation aligns with previous evidence implicating PLR as a surrogate marker of immune-thrombotic dysregulation [19], though our study is the first to quantify its threshold effects in PAH. Subgroup analyses reinforced the robustness of PLR's prognostic value, showing consistent mortality gradients across age, sex, and comorbidity strata without significant interaction effects. The heightened mortality observed in CKD and COPD subgroups, although not significantly modified, may reflect amplified systemic inflammation in these populations [15,19].

From a methodological perspective, exclusion of collinear variables (e.g., hematocrit) preserved model integrity, with retained predictors (PLR and SOFA score) demonstrating low multicollinearity. The adjusted Cox model achieved a C-index of 0.733, indicating clinically meaningful predictive accuracy, while machine learning-derived risk scores provide an additional framework for personalized mortality risk assessment.

This study has several limitations. First, its retrospective design introduces inherent biases and potential unmeasured confounders. Second, reliance on single-timepoint PLR measurements precluded longitudinal assessment of dynamic changes. The lack of granular PAH-specific parameters, such as right ventricular function metrics, further limits mechanistic insights into the role of PLR in pulmonary vascular remodeling [22,23]. Additionally, the fixed-time hematologic sampling in MIMIC-IV precluded evaluation of PLR trajectory changes relative to evolving clinical outcomes. Future prospective studies should validate these thresholds in diverse populations with protocol-driven blood sampling and investigate whether targeted interventions that modulate PLR across disease phases can improve outcomes.

5. Conclusion

PLR emerges as a pragmatic, easily obtainable biomarker for mortality risk stratification in critically ill PAH patients. Identification of specific PLR thresholds (67.32–75.92) offers actionable targets for prognostic assessment, facilitating earlier recognition of high-risk patients. Integration of PLR into existing prognostic models could enhance predictive accuracy and optimize resource allocation in critical care settings, though clinical decisions regarding monitoring or therapeutic strategies should remain individualized and based on comprehensive evaluation.

Key Points

• PLR demonstrates a U-shaped relationship with 28-day mortality in critical PAH, with risk increasing beyond 67.32 and relatively reduced below this threshold (adjusted HR = 3.787, 95% CI: 2.431–5.898).

• Defined PLR thresholds (67.32–75.92) enable rapid ICU risk stratification using routine admission blood tests.

• Machine learning confirmed the contribution of PLR to mortality prediction (AUC = 0.759), with each unit increase in PLR associated with a 19.8% rise in risk.

• Elevated PLR predicted mortality consistently across age, sex, CKD, and COPD subgroups without significant interaction effects.

Availability of Data and Materials

The data analyzed in this study comes from the publicly available MIMIC-IV database, but the use of the data has certain restrictions and requires training and permission. The research data can be found at the following URL: https://mimic.mit.edu/.

Author Contributions

Conceptualization, DDG and ZGZ; methodology, DDG; software, DDG; validation, DDG, ZGZ; formal analysis, DDG; investigation, DDG; resources, DDG, ZGZ; data curation, DDG; writing—original draft preparation, DDG; visualization, DDG; supervision, ZGZ; project administration, ZGZ. Both authors contributed to revising the manuscript critically for important intellectual content. Both authors have read and agreed to the final published version of the manuscript. Both authors have participated sufficiently in the work and agreed to be accountable for all aspects of the work.

Ethics Approval and Consent to Participate

This study is a retrospective analysis based on the de-identified Medical Information Mart for Intensive Care IV (MIMIC-IV) database. As the database has already undergone ethical review and obtained informed consent waiver from the Institutional Review Board (IRB) of Beth Israel Deaconess Medical Center, no additional ethical approval or informed consent is required for the present study.

Acknowledgment

The authors express gratitude to the participants involved in the MIMIC-IV database and all related researchers.

Funding

This research received no external funding.

Conflict of Interest

The authors declare no conflict of interest.

Supplementary Material

Supplementary material associated with this article can be found, in the online version, at https://doi.org/10.31083/BJHM52966.

References

[1] Balistrieri A, Makino A, Yuan JXJ. Pathophysiology and pathogenic mechanisms of pulmonary hypertension: role of membrane receptors, ion channels, and Ca^{2+} signaling. Physiological Reviews. 2023; 103: 1827–1897. https://doi.org/10.1152/physrev.00030.2021.

[2] Satoh T. Current practice for pulmonary hypertension. Chinese Medical Journal. 2014; 127: 3491–3495.

[3] Satoh T. Pulmonary hypertension: a review of current clinical practice. Zhonghua Xin Xue Guan Bing Za Zhi. 2014; 42: 450–452. (In Chinese)

[4] Escribano Subias P, Barberà Mir JA, Suberviola V. Current diagnostic and prognostic assessment of pulmonary Hypertension. Revista Espanola De Cardiologia. 2010; 63: 583–596. https://doi.org/10.1016/s1885-5857(10)70120-1.

[5] Galiè N, Humbert M, Vachiery JL, Gibbs S, Lang I, Torbicki A, *et al*. 2015 ESC/ERS Guidelines for the diagnosis and treatment of pulmonary hypertension: The Joint Task Force for the Diagnosis and Treatment of Pulmonary Hypertension of the European Society of Cardiology (ESC) and the European Respiratory Society (ERS): Endorsed by: Association for European Paediatric and Congenital Cardiology (AEPC), International Society for Heart and Lung Transplantation (ISHLT). European Heart Journal. 2016; 37: 67–119. https://doi.org/10.1093/eurheartj/ehv317.

[6] Iancu DG, Mares RG, Cristescu L, Suteu RA, Varga A, Tilea I. Inflammation-Based Hematologic Indices as Prognostic Markers in Pulmonary Arterial and Chronic Thromboembolic Pulmonary Hypertension: A Hypothesis-Generating Registry Study. International Journal of Molecular Sciences. 2025; 26: 10940. https://doi.org/10.3390/ijms262210940.

[7] Wang RR, Yuan TY, Wang JM, Chen YC, Zhao JL, Li MT, *et al*. Immunity and inflammation in pulmonary arterial hypertension: From pathophysiology mechanisms to treatment perspective. Pharmacological Research. 2022; 180: 106238. https://doi.org/10.1016/j.phrs.2022.106238.

[8] Hojda SE, Chis IC, Clichici S. Biomarkers in Pulmonary Arterial Hypertension. Diagnostics. 2022; 12: 3033. https://doi.org/10.3390/diagnostics12123033.

[9] Uzun F, Erturk M, Cakmak HA, Kalkan AK, Akturk IF, Yalcin AA, *et al*. Usefulness of the platelet-to-lymphocyte ratio in predicting long-term cardiovascular mortality in patients with peripheral arterial occlusive disease. Advances in Interventional Cardiology. 2017; 13: 32–38. https://doi.org/10.5114/aic.2017.66184.

[10] Serra R, Ielapi N, Licastro N, Provenzano M, Andreucci M, Bracale UM, *et al*. Neutrophil-to-lymphocyte Ratio and Platelet-to-lymphocyte Ratio as Biomarkers for Cardiovascular Surgery Procedures: A Literature Review. Reviews on Recent Clinical Trials. 2021; 16: 173–179. https://doi.org/10.2174/1574887115999201027145406.

[11] Zhai G, Wang J, Liu Y, Zhou Y. Platelet-lymphocyte ratio as a new predictor of in-hospital mortality in cardiac intensive care unit patients. Scientific Reports. 2021; 11: 23578. https://doi.org/10.1038/s41598-021-02686-1.

[12] Simonneau G, Montani D, Celermajer DS, Denton CP, Gatzoulis MA, Krowka M, *et al*. Haemodynamic definitions and updated clinical classification of pulmonary hypertension. The European Respiratory Journal. 2019; 53: 1801913. https://doi.org/10.1183/13993003.01913-2018.

[13] Singer M, Deutschman CS, Seymour CW, Shankar-Hari M, Annane D, Bauer M, *et al*. The Third International Consensus Definitions for Sepsis and Septic Shock (Sepsis-3). JAMA. 2016; 315: 801–810. https://doi.org/10.1001/jama.2016.0287.

[14] Rodriguez-Arias JJ, García-Álvarez A. Sex Differences in Pulmonary Hypertension. Frontiers in Aging. 2021; 2: 727558. https://doi.org/10.3389/fragi.2021.727558.

[15] Gaddam S, Gunukula SK, Lohr JW, Arora P. Prevalence of chronic kidney disease in patients with chronic obstructive pulmonary disease: a systematic review and meta-analysis. BMC Pulmonary Medicine. 2016; 16: 158. https://doi.org/10.1186/s12890-016-0315-0.

[16] Hu X, Cheng S, Du H, Yin Y. Association of platelet-to-lymphocyte ratio with 1-year all-cause mortality in ICU patients with heart failure. Scientific Reports. 2024; 14: 32016. https://doi.org/10.1038/s41598-024-83583-1.

[17] Shahane A. Pulmonary hypertension in rheumatic diseases: epidemiology and pathogenesis. Rheumatology International. 2013; 33: 1655–1667. https://doi.org/10.1007/s00296-012-2659-y.

[18] Kilickiran Avci B, Basarici I, Akbulut M, Atas H, Yaylali YT, Sinan UY, *et al*. Comorbidity Burden in Chronic Thromboembolic Pulmonary Hypertension: Implications and Outcome. Medicina. 2025; 61: 827. https://doi.org/10.3390/medicina61050827.

[19] Bi W, Liu Y, Wu W, Lian S, Pei Z, Zhu F, *et al*. Association of nine composite inflammatory indices with cardiovascular diseases in US adults: national health and nutrition examination survey (NHANES, 2005-2018). Journal of Health, Population, and Nutrition. 2026; 45: 55. https://doi.org/10.1186/s41043-025-01222-5.

[20] Price LC, Wort SJ, Perros F, Dorfmüller P, Huertas A, Montani D, *et al*. Inflammation in pulmonary arterial hypertension. Chest. 2012; 141: 210–221. https://doi.org/10.1378/chest.11-0793.

[21] Balta S, Ozturk C. The platelet-lymphocyte ratio: A simple, inexpensive and rapid prognostic marker for cardiovascular events. Platelets. 2015; 26: 680–681. https://doi.org/10.3109/09537104.2014.979340.

[22] Steppan J, Wang H, Nandakumar K, Gadkari M, Poe A, Pak L, *et al*. LOXL2 inhibition ameliorates pulmonary artery remodeling in pulmonary hypertension. American Journal of Physiology. Lung Cellular and Molecular Physiology. 2024; 327: L423–L438. https://doi.org/10.1152/ajplung.00327.2023.

[23] Weir-McCall JR, Liu-Shiu-Cheong PS, Struthers AD, Lipworth BJ, Houston JG. Pulmonary arterial stiffening in COPD and its implications for right ventricular remodelling. European Radiology. 2018; 28: 3464–3472. https://doi.org/10.1007/s00330-018-5346-x.